Generation of multicolor vacuum ultraviolet pulses through four-wave sum-frequency mixing in argon

Liping Shi,[1] Wenxue Li,[1,*] Hui Zhou,[1] Di Wang,[1] Liang'en Ding,[1] and Heping Zeng[1,2,†]

[1]*State Key Laboratory of Precision Spectroscopy, East China Normal University, Shanghai 200062, China*

[2]*Shanghai Key Laboratory of Modern Optical System, Engineering Research Center of Optical Instrument and System, Ministry of Education, School of Optical-Electrical and Computer Engineering, University of Shanghai for Science and Technology, Shanghai 200093, China*

(Received 16 July 2013; published 18 November 2013)

We demonstrate efficient generation of multicolor vacuum ultraviolet pulses with excellent mode quality through $\chi^{(3)}$-based four-wave sum-frequency mixing and third-order harmonic generation of 400- and 267-nm femtosecond laser pulses in argon gas. The $\chi^{(3)}$-based nonlinear optical processes were optimized with appropriate control of gas pressure and group velocity delay between the driving pulses. Furthermore, the pulse breakup effects were observed for tightly focused ultraviolet pulses.

DOI: 10.1103/PhysRevA.88.053825 PACS number(s): 42.65.Re, 42.65.Ky, 52.38.Hb

I. INTRODUCTION

For experimental investigations in the formation and dissociation dynamics of molecular superexcited states [1], laser-induced precision spectroscopy [2], as well as laser-induced micro- and nanomachining [3], ultrashort energetic vacuum ultraviolet (VUV) pulses are desired due to the relatively high photon energies and small diffraction limit in this spectral domain. Yet, the restricted transparent range and high dispersion of solid media limit the use of birefringent crystals to generate ultrashort VUV laser pulses. The shortest wavelength achieved so far was 156 nm; this was done by using $KBe_2BO_3F_2$ crystals [4]. On the other hand, despite their low nonlinearities, noble gaseous media have been demonstrated as excellent alternatives to generate VUV wavelengths owing to their low dispersion and transmission in a wide range of wavelengths. Sufficient harmonic conversion could be achieved by interacting high-intensity pump laser sources in gaseous media with extended phase-matched lengths. For instance, cascaded nonlinear wave mixing in hollow fiber filled with noble gases was controlled to support broad-bandwidth phase-matched frequency conversion into deep-ultraviolet (DUV) and VUV regions [5]. Filamentary propagation of intense ultrashort pulses in air allowed long-distance self-phase-matched third-harmonic generation [6] in DUV, which was further enhanced by external disturbance [7], such as laser-induced plasma [8–11], droplet water [12], and gas pressure gradient [13]. With self-generated plasma channels to balance Kerr self-focusing, femtosecond filaments could propagate much longer than the Rayleigh range with the typical clamping intensity of 10^{13}–10^{14} W/cm^2 [14], bringing about dramatic enhancement of nonlinear optical processes such as four-wave mixing (FWM) or direct high harmonic [15] in the filamentary zone. Self-channeled FWM during filamentation of near-infrared and infrared laser pulses in air and argon was demonstrated to support efficient generation of tunable and stable ultrashort laser pulses in the visible spectrum with high conversion efficiency, low fluctuation, and excellent beam mode quality [16]. By mixing fundamental-wave (FW, ω) and its second-harmonic (SH, 2ω) filaments in neon gas, efficient third-harmonic (TH, 3ω) and fourth-harmonic (FH 4ω) pulses were achieved [17,18]. By four-wave difference-frequency mixing between 800-nm Ti:sapphire FW and TH pulses, the fifth harmonic (5ω) at 160 nm was produced in argon gas [19,20]. On the other hand, using near-resonant two-photon-excitation-based difference-frequency FWM in xenon gas, Tünnermann *et al*. demonstrated the generation of tunable picoseconds VUV pulses with the wavelength down to 133 nm [21], which was the shortest wavelength for intense femtosecond VUV pulses achieved so far. Further generation of femtosecond VUV pulses with shorter wavelength is limited by the absence of intense DUV pumping laser sources.

In this paper, we demonstrate a $\chi^{(3)}$-based four-wave sum-frequency mixing and third-order harmonic generation scheme between two energetic DUV (SH, 2ω; TH, 3ω) femtosecond pulses in argon gas to achieve energetic multicolor VUV pulse generation at 200, 133, 114, 100, and 89 nm, corresponding to harmonics of 4ω, 6ω, 7ω, 8ω, and 9ω. The nonlinear coupling between these fields is essential to investigate filamentary propagation of multicolor VUV pulses in gaseous media.

II. EXPERIMENTAL RESULTS AND DISCUSSION

The experiments were performed with a Ti:sapphire multipass amplified laser system producing 800-nm pulses with energies per pulse up to 50 mJ. The FW was split into two equal beams, as shown in Fig. 1. One passed through a beta-barium borate (BBO) crystal (type I) for the SH generation (2ω). The energy of the 2ω pulse was ~5 mJ. The other FW beam passed through three BBO crystals to generate its TH pulse (3ω), with the pulse energy up to ~1.5 mJ [22,23]. The pulse duration of the generated 2ω and 3ω harmonics was estimated to be about 100 fs. The polarizations of the 2ω and 3ω pulses were rotated parallel to each other. These dual-color ultraviolet pulses were then recombined by a dichroic mirror to form a collinear beam. Their time delay ($\Delta\tau$) could be adjusted with an optical delay line. Two concave mirrors, with equal focal lengths $f = 250$ mm, were introduced to independently focus the two-color pulses into a stainless steel gas cell through a 0.2-mm-thick fused silica Brewster window. Argon gas flowed into the gas cell with controllable pressures. In this way, a two-color plasma channel with the typical length of ~2 cm

*wxli@phy.ecnu.edu.cn
†hpzeng@phy.ecnu.edu.cn

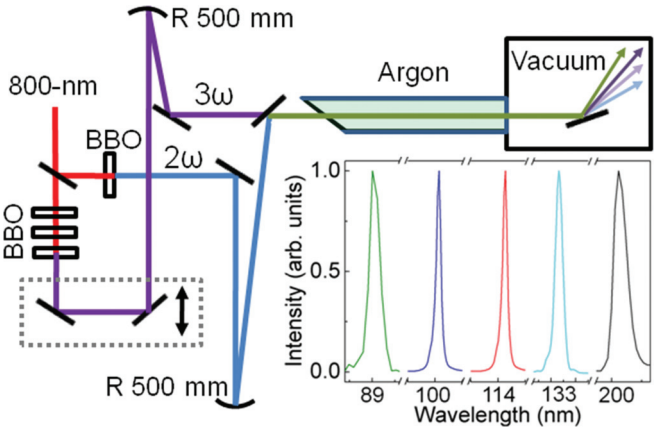

FIG. 1. (Color online) Schematic illustration of experimental setup for multicolor VUV pulses generation from four-wave sum-frequency mixing of 266-nm and 400-nm femtosecond pulses in argon. Argon gases flowed into the gas cell flowed at various pressures and the subsequent VUV CCD was separated by a 0.1-mm-thick copper sheet. The inset photograph shows the generated spectral signals of multicolor VUV pulses.

was produced. A 0.1-mm-thick copper sheet with a ∼100-μm laser-drilled pinhole was utilized to seal up the end of the gas cell, which transmitted the generated VUV pulses to the vacuum chamber. The background pressure was maintained at less than 0.1 mbar. The VUV generation from FWM between 2ω and 3ω pulses was collected with a spherical mirror located about 50 cm away from the pinhole and further monitored by a combination of McPherson monochromator and VUV-optimized Andor charge-coupled device (CCD) camera.

The inset of Fig. 1 gives the spectra of harmonics generated via FWM processes of synchronized 2ω and 3ω pulses during their copropagation. Each of the spectral signals was independently normalized, and was close to Gaussian distribution. The outputs of 6ω (∼133 nm, curve IV) and 9ω (∼89 nm, curve I) pulses were assigned to the TH generation during the filamentation of 2ω and 3ω pulses. Note that the $3p \rightarrow 3d$ transition of neutral argon atom is near resonant with three-photon excitation of the 3ω pulse. Consequently, remarkably efficient generation of 89 nm, i.e., the third harmonic of 3ω, may partly benefit from the resonantly enhanced nonlinear susceptibility. The outputs of the 7ω (curve III) and 8ω (curve II) components centered at ∼114 and ∼100 nm originated from the sum-frequency FWM processes $3\omega + 2\omega + 2\omega \rightarrow 7\omega$, $3\omega + 3\omega + 2\omega \rightarrow 8\omega$, respectively, and the 4ω (∼200 nm, curve V) harmonic stemmed from difference-frequency FWM $3\omega + 3\omega - 2\omega \rightarrow 4\omega$. These multicolor ultraviolet fields were strongly coupled with each other during the FWM processes, with efficient energy exchange within the entire interaction region, resulting in intense VUV pulse generation and multicolor filamentation in argon gas that facilitated cross-interaction among these VUV fields, which significantly increased the length and brightness of the filament column.

In order to better understand the difference-frequency FWM processes, we first investigated 200-nm pulse generation in ambient air. We employed five 200-nm highly reflective mirrors to extract it from the pump lights and record its

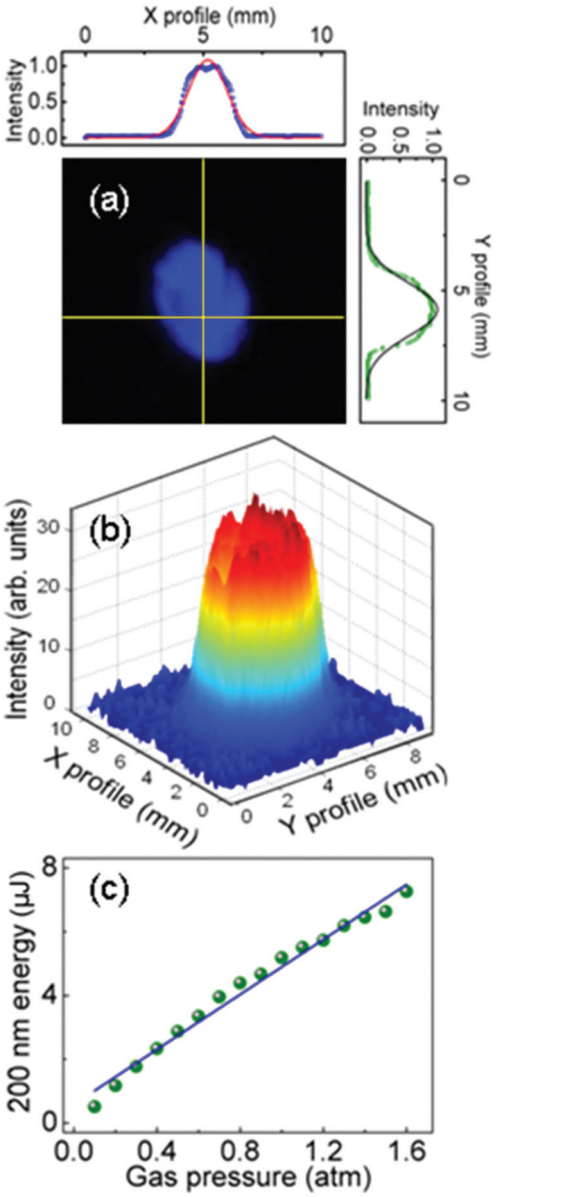

FIG. 2. (Color online) (a) Experimentally observed far-field image and its intensity distribution along the X and Y profiles. The red (upper) and black (right) curves are Gaussian fitting results. (b) Three-dimensional intensity distribution of the generated 200-nm pulse through the difference-frequency FWM. (c) The dependence of the 200-nm pulse energy on argon gas pressure.

energy as well as its beam profile. The maximal energy of the generated 200-nm pulse was measured to be 2.8 μJ by a powermeter, with its far-field image and intensity distribution of beam profile depicted in Figs. 2(a) and 2(b), respectively. The beam profile was smooth and close to typically symmetric Gaussian distribution. Interestingly, even these two initially incident pump beams were tailored to asymmetric distribution, such as square or even triangular; we found that the excellent beam profile of the output 200-nm pulse was robust. This verified the spatial self-cleaning effect during the formation of a self-generated plasma channel [24]. Since the FWM processes occurred inside the high-intensity nonlinearly focusing core region of circular symmetry, the beam profile of

generated harmonics was independent of the initial energy reservoir distribution of the pump beam. However, the beam profiles of the VUV pulses were undiscovered because we have no reflective mirrors for the extraction of those that had propagated in the vacuum chamber.

We were then concerned with the conversion efficiency of the 200-nm pulse in argon gas at various pressures, as shown in Fig. 2(c). The generated 200-nm pulse energy was linearly rather than quadratically increased with the gas pressure. This occurred because the filament volume, which was inversely proportional to the gas pressure, linearly reduced the high-intensity core for the harmonic generation. The maximum output energy of the 200-nm pulse was 7.6 μJ. The conversion efficiency was approximately 0.5% of the 3ω beam. Note that the highest gas pressure we could acquire inside the gas cell was 1.6 atm. A higher FWM conversion efficiency was obtained in argon gas than that in air, in spite of their similar third-order susceptibility. This could be understood as being due to the higher filamentation clamping intensity in argon gas [25–27]. However, regardless of the even higher clamping intensities in neon and helium gases, the harmonic conversion efficiency was measured to be lower than that in argon gas. This should be ascribed to the relatively low third-order susceptibilities of neon and helium gases.

We further examined the dependence of 7ω (black squares) and 8ω (blue circles) harmonic generation on argon gas pressure, as shown in Fig. 3(a). In this case, the driving 2ω and 3ω pump pulses were adjusted to be synchronized. We obtained the highest output pulse energy of up to 1.8 μJ at a pressure of 0.1 atm for 7ω, with a rapid attenuation at lower pressures, while decreasing gradually towards higher pressures. Similarly, the 8ω pulse generation peaked at 0.08 atm, with the highest pulse energy of 1.6 μJ. It should be pointed out that a direct measurement of the VUV pulse energy was limited by using a standard powermeter. We, instead, approximately measured the 7ω and 8ω pulse energies according to their integrated spectral intensity ratio with respect to the 200-nm pulse, i.e., $E_A = E_{4\omega} I_{sp}^{A} / I_{sp}^{4\omega}$ (A stands for 7ω or 8ω). The estimated accuracy of the VUV pulse energies was $\sim$0.1 μJ. The spectra of 7ω and 8ω pulses had a full width at half maximum (FWHM) of 0.25 and 0.21 nm, respectively, which would permit Fourier-transform-limited pulse duration of 70 and 76 fs, respectively.

The observed pressure-dependent harmonic conversion efficiency could be understood by phase-matching in self-guided

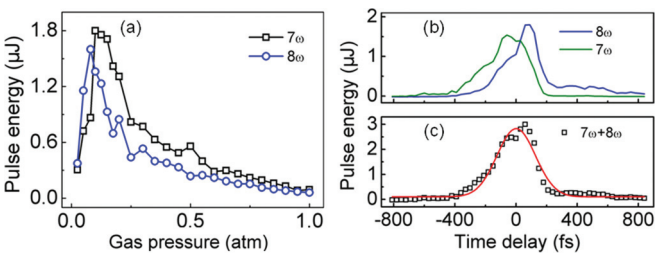

FIG. 3. (Color online) Experimentally measured dependence of 7ω (olive curve or curve I) and 8ω (blue curve or curve II) harmonics on argon gas pressure (a), and on the time delay between 2ω and 3ω driving pulses (b). The sum energy of 7ω and 8ω pulses as a function of the time delay (c).

plasma filament. Due to the free-electron-induced refractive index variation, the k-vector of the generated harmonic is [28]

$$k_{q\omega} = \frac{2q\pi[n_{q\omega}(1-\eta) - N_e/2q^2N_c]}{\lambda}, \tag{1}$$

where q and $n_{q\omega}$ denote the harmonic order and corresponding refraction index at $q\omega$, η is ionization rate, N_e is the electron density, which was measured to be $\sim 2 \times 10^{17}$ cm^{-3} based on an in-line holographic imaging technique [29], and $N_c = 1.7 \times 10^{21}$ cm^{-3} represents the critical plasma density for wavelength $\lambda \sim 800$ nm. Phase-matching condition $\Delta k \sim 0$ could be achieved through gas pressure control. The optimal gas pressure P for phase-matched harmonic conversion takes the form [19]

$$P \sim \lambda / \left| \pi w_0^2 n_{2\omega} \Delta k_0 \right|, \tag{2}$$

where the gas pressure P is measured in atmospheres, w_0 denotes the laser beam waist, Δk_0 represents the pressure-dependent total phase mismatch between generated harmonic and pumping sources at 1 atm pressure. Here, we have $\Delta k_0 = k_{4\omega} + k_{2\omega} - 2k_{3\omega} = 3.12$ cm^{-1} for 4ω, $\Delta k_0 = k_{7\omega} - 2k_{2\omega} - k_{3\omega} = 63.9$ cm^{-1} for 7ω, and $\Delta k_0 = k_{8\omega} - k_{2\omega} - 2k_{3\omega} = 92.4$ cm^{-1} for 8ω. The refractive index for each harmonic was taken from Ref. [30]. The optimal gas pressure for harmonic generation was estimated to be $P \sim 2$ atm for 4ω, $P \sim 0.1$ atm for 7ω, and $P \sim 0.07$ atm for 8ω, respectively. The theoretically calculated values are in excellent agreement with the aforementioned experimental results.

Figure 3(b) shows the intensity of generated 7ω and 8ω harmonics as a function of time delay between 2ω and 3ω pulses, while the gas pressure was maintained at 0.9 atm. Here, positive delays $\Delta\tau > 0$ are stipulated for 2ω pulses launched ahead of 3ω pulses. By monitoring the generated VUV harmonic intensities at various time delays, we found that the 3ω pulse should be retarded by about 40 fs rather than synchronized with respect to the 2ω pulse for the highest conversion efficiency of 8ω harmonic pulse. At zero delay, the dramatic competition between the 7ω and 8ω generation halved the conversion efficiency of each FWM process, while the total harmonic energy was still maximized, as shown in Fig. 3(c). The optimal generation of the 8ω harmonics at the delay of 40 fs might be originated from the driving-pulse splitting effect during the filamentation process. Inside the self-guiding plasma channel, due to all sorts of highly nonlinear effects, the intense laser pulse underwent considerable spatial-temporal deformation, resulting in spatiotemporal reshaping of the copropagating pulses [14]. The initial driving pulse broke up into a dominant pulse following by a long subpulse [31]. The phase of the 8ω harmonic was mainly locked with the 3ω pulse because it was a higher-order process with respect to the 3ω pulse. In the case of positive delay, the intense dominant pulse of 3ω caught up with the trailing edge of the 2ω pulse envelope, leading to the primary generation of the 8ω harmonic ($3\omega + 3\omega + 2\omega \rightarrow 8\omega$). Interestingly, at large time delays ranging from 200 to 600 fs, there still existed obvious 8ω harmonic components. This could be attributed to the four-wave mixing between the leading pulse of 3ω and disrupted weak subpulses of 2ω. However, no 8ω harmonic was observed at corresponding negative delays, which confirmed the aforementioned phase-locking mechanism. Likewise, the

7ω harmonic represented an inverse tendency, i.e., its intensity peaked at $\Delta\tau \sim -40$ fs and gradually declined towards negative delays.

III. CONCLUSION

In conclusion, we have demonstrated efficient generation of multicolor VUV laser pulses via FWM processes between two tightly focusing UV femtosecond laser pulses in argon. The experiments showed that the generated ultraviolet pulses exhibited excellent mode qualities as a result of self-filtering inside the filaments. This method could be extended for the generation of few-cycle wavelength-tunable laser sources in the VUV spectral range by employing an optical parametric amplifier, allowing further investigations in ultraviolet nonlinear optics, time-resolved spectroscopic studies, and other interdisciplinary applications in ultrafast science.

ACKNOWLEDGMENTS

We acknowledge financial support from the National Basic Research Program of China (Grant No. 2011CB808105), National Key Scientific Instrument Project (Grant No. 2011YQ150072), National Natural Science Fund of China (Grants No. 11004061, No. 11274115, and No. 10990101), and International Science and Technology Collaboration Program (Grants No. 2010DFA04410 and No. 11530700900). Liping Shi thanks the Fostering Project for National Top Hundred Doctoral Dissertations of ECNU (Grant No. PY2012010).

[1] H. Timmers, N. Shivaram, and A. Sandhu, Phys. Rev. Lett. **109**, 173001 (2012).
[2] I. V. Hertel and W. Radloff, Rep. Prog. Phys. **69**, 1897 (2006).
[3] D. Kiselev, L. Woeste, and J. P. Wolf, Appl. Phys. B **100**, 515 (2010).
[4] T. Kanai, T. Kanda, T. Sekikawa, S. Watanabe, T. Togashi, C. Chen, C. Zhang, Z. Xu, and J. Wang, J. Opt. Soc. Am. B **21**, 370 (2004).
[5] L. Misoguti, S. Backus, C. G. Durfee, R. Bartels, M. M. Murnane, and H. C. Kapteyn, Phys. Rev. Lett. **87**, 013601 (2001).
[6] N. Aközbek, A. Iwasaki, A. Becker, M. Scalora, S. L. Chin, and C. M. Bowden, Phys. Rev. Lett. **89**, 143901 (2002).
[7] Y. Liu, M. Durand, A. Houard, B. Forestier, A. Couairon, and A. Mysyrowicz, Opt. Commun. **284**, 4706 (2011).
[8] K. Hartinger and R. A. Bartels, Appl. Phys. Lett. **93**, 151102 (2008).
[9] S. Suntsov, D. Abdollahpour, D. G. Papazoglou, and S. Tzortzakis, Opt. Express **17**, 3190 (2009).
[10] X. Yang, J. Wu, Y. Peng, Y. Tong, S. Yuan, L. Ding, Z. Xu, and H. Zeng, Appl. Phys. Lett. **95**, 111103 (2009).
[11] S. Suntsov, D. Abdollahpour, D. G. Papazoglou, and S. Tzortzakis, Phys. Rev. A **81**, 033817 (2010).
[12] T. Xi, X. Lu, and J. Zhang, Opt. Commun. **282**, 3140 (2009).
[13] E. Schulz, D. S. Steingrube, T. Vockerodt, T. Binhammer, U. Morgner, and M. Kovačev, Opt. Lett. **36**, 4389 (2011).
[14] A. Couairon and A. Mysyrowicz, Phys. Rep. **441**, 47 (2007).
[15] D. S. Steingrube, E. Schulz, T. Binhammer, M. B. Gaarde, A. Couairon, U. Morgner, and M. Kovačev, New J. Phys. **13**, 043022 (2011).
[16] F. Théberge, N. Aközbek, W. Liu, A. Becker, and S. L. Chin, Phys. Rev. Lett. **97**, 023904 (2006).
[17] T. Fuji, T. Horio, and T. Suzuki, Opt. Lett. **32**, 2481 (2007).
[18] T. Fuji, T. Suzuki, E. E. Serebryannikov, and A. Zheltikov, Phys. Rev. A **80**, 063822 (2009).
[19] M. Beutler, M. Ghotbi, F. Noack, and I. V. Hertel, Opt. Lett. **35**, 1491 (2010).
[20] M. Beutler, M. Ghotbi, and F. Noack, Opt. Lett. **36**, 3726 (2011).
[21] A. Tünnermann, C. Momma, K. Mossavi, C. Windolph, and B. Wellegehausen, IEEE J. Quantum Electron. **29**, 1233 (1993).
[22] L. Shi, W. Li, Y. Wang, X. Lu, L. Ding, and H. Zeng, Phys. Rev. Lett. **107**, 095004 (2011).
[23] L. Shi, W. Li, H. Zhou, D. Wang, L. Ding, and H. Zeng, Appl. Phys. Lett. **102**, 081112 (2013).
[24] B. Prade, M. Franco, A. Mysyrowicz, A. Couairon, H. Buersing, B. Eberle, M. Krenz, D. Seiffer, and O. Vasseur, Opt. Lett. **31**, 2601 (2006).
[25] A. Couairon, H. S. Chakraborty, and M. B. Gaarde, Phys. Rev. A **77**, 053814 (2008).
[26] A. Couairon and L. Bergé, Phys. Rev. Lett. **88**, 135003 (2002).
[27] W. Ettoumi, Y. Petit, J. Kasparian, and J. P. Wolf, Opt. Express **18**, 6613 (2010).
[28] T. Popmintchev, M. Chen, A. Bahabad, M. Gerrity, P. Sidorenko, O. Cohen, I. P. Christov, M. M. Murnane, and H. C. Kapteyn, Proc. Natl. Acad. Sci. USA **106**, 516 (2009).
[29] M. Durand, A. Jarnac, Y. Liu, B. Prade, A. Houard, V. Tikhonchuk, and A. Mysyrowicz, Phys. Rev. E **86**, 036405 (2012).
[30] E. R. Peck and J. D. Fisher, J. Opt. Soc. Am. **54**, 1362 (1964).
[31] S. Tzortzakis, B. Lamouroux, A. Chiron, S.D. Moustaizis, D. Anglos, M. Franco, B. Prade, and A. Mysyrowicz, Opt. Commun. **197**, 131 (2001).